

Two-dimensional clusters of liquid ^4He

A. Sarsa

Dept. de Física Moderna, Universidad de Granada, E-18071 Granada, Spain
International School for Advanced Studies,
SISSA, Via Beirut 2/4, I-34014, Trieste, Italy

J. Mur-Petit, A. Polls

Dept. d'Estructura i Constituents de la Matèria,
Universitat de Barcelona, Diagonal, 647, E-08028 Barcelona, Spain

J. Navarro

IFIC, CSIC-Universitat de València,
Apdo. 20285, E-46071 València, Spain

(Dated: February 7, 2020)

Abstract

The binding energies of two-dimensional clusters (puddles) of ^4He are calculated in the framework of a linear diffusion Monte Carlo method. The results are very well fitted by a mass formula in powers of $x = N^{-1/2}$, where N is the number of particles. The analysis of the mass formula allows for the extraction of the line tension, which turns out to be $0.121 \text{ K}/\text{\AA}$. Sizes and density profiles of the puddles are also reported.

PACS numbers: 36.40.-c 61.46.+w 67.70.+n

I. INTRODUCTION

In recent years, a great deal of work has been devoted to study quantum liquids in restricted geometries.¹ One important feature of these systems is that their internal structure becomes more easily observable than in bulk liquids due to the restricted motion of the particles in the confining potential. Among these systems the study of quantum films has received particular attention. They consist of liquid helium adsorbed to a more-or-less attractive flat surface. In 1973 M. Bretz *et al.*² observed for the first time the adsorption of ⁴He onto the basal plane of graphite. In the last few years, adsorption properties of helium on different substrates such as carbon, alkali and alkaline-earth flat surfaces, carbon nanotubes and aerogels have become a fertile topic of research.

The structure and growth of thin films of ⁴He adsorbed to a substrate was studied by Clements *et al.*³ employing the optimized hypernetted-chain Euler-Lagrange theory with realistic atom-atom interactions. It turns out that films with low surface coverages, where all atoms cover the surface with a thickness corresponding to a single atom, can be approximated reasonably well by a 2D model. In connection with these systems, an interesting question naturally arises as how physics depends on the dimensionality of the space.

The homogeneous 2D liquid has been studied using different theoretical methods, such as molecular dynamics⁴ and quantum Monte Carlo simulations either Green's Function⁵ or diffusion⁶ techniques. The inhomogeneous case was studied by Krishnamachari and Chester,⁷ who used a shadow variational wave function to describe 2D puddles of liquid ⁴He. In this work we report energies and density profiles of puddles calculated within the diffusion Monte Carlo (DMC) method. Our main objective is to give an accurate estimate of the line energy or the line tension of the 2D liquid ⁴He. As atom-atom interaction we have used the revised version of the Aziz potential dubbed as HFD-B(HE).⁸ This potential has been used to study ground-state properties of 3D bulk ⁴He and ³He,^{9,10} within the DMC framework, and it has proved to accurately reproduce the ground-state properties of both liquids at zero temperature.

The trial wave function used for the importance sampling in the DMC calculation is introduced in Section II, where the variational Monte Carlo results for this wave function are also reported. A brief explanation of the DMC techniques used in the present paper is presented in Section III. Section IV contains the DMC results and their analysis in terms

of a mass formula in 2D. The line tension is extracted from this mass formula. Properties characterizing the puddles, such as the density profiles, are discussed in Section V. Finally, the main conclusions are summarized in Section VI.

II. VARIATIONAL GROUND-STATE ENERGIES

To study a system of N ^4He atoms in two dimensions we start from the following trial wave function

$$\Phi_T(\mathbf{R}) = \prod_{i < j} \exp \left[-\frac{1}{2} \left(\frac{b}{r_{ij}} \right)^\nu - \frac{\alpha^2}{2N} r_{ij}^2 \right], \quad (1)$$

written in the same way as in the 3D case.¹¹ The coordinate \mathbf{R} indicates the set of coordinates of all the particles $\{\mathbf{r}_1, \mathbf{r}_2, \dots, \mathbf{r}_N\}$, while r_{ij} stands for the interparticle distance, $r_{ij} = |\mathbf{r}_j - \mathbf{r}_i|$. The trial wave function contains the simple McMillan form¹² to deal with the very short-range part of the interaction, and the translationally invariant part of a harmonic oscillator (HO) wave function with parameter α , to roughly confine the system.

In our calculations the value $\hbar^2/m_4 = 12.1194$ K Å² has been employed for the atom mass and the parameters b and ν have been fixed to the values 3.00 Å and 5, respectively, the same values as in 3D calculations. The variational search has thus been restricted to the HO parameter α , whose optimal value is given in Table I. The expectation value of the Hamiltonian, as well as the separate contributions of kinetic and potential energies are given in the same Table for puddles with N atoms. It can be seen that the total energy results from an important cancellation between kinetic and potential energies, which is in fact larger than in the 3D case. Let us recall that in 3D bulk, the energy per particle results from adding ≈ 14 K of kinetic energy with ≈ -21 K of potential energy. In 2D, both kinetic and potential contributions are very close to each other, which makes the calculation very delicate.

In the last column of Table I the VMC results of Krishnamachari and Chester⁷ are reported. As compared with their results, our calculations provide smaller binding energies, in spite of the fact that the interaction used in Ref. 7 is an older version of the Aziz potential, which tends to underbind the systems. In fact, the shadow wave function used in Ref. 7 contains more elaborated correlations not present in our simple trial wave function. The VMC energy for the bulk system corresponds to the saturation density, $\rho_0 = 0.04344$ Å⁻², taken from the DMC calculation of Ref. 6.

We have also performed calculations using a different trial wave function, replacing the translationally invariant gaussian part by an exponential one, i.e.

$$\Phi_T(\mathbf{R}) = \prod_{i < j} \exp \left[-\frac{1}{2} \left(\frac{b}{r_{ij}} \right)^\nu - \frac{\alpha}{2} r_{ij} \right], \quad (2)$$

expecting that this larger tail in the wave function will result in more binding. Actually, we do not find significant differences for small values of N . For instance, in the case $N = 8$, using the same values for b and ν as before, we get $E/N = -0.2178(5)$ K, $T/N = 1.266(2)$ K, $V/N = -1.484(2)$ K for $\alpha = 0.035 \text{ \AA}^{-1}$. When the values of b , ν and α are optimized, we obtain a slightly larger binding energy, $E = -0.2267(8)$ K for $b = 3.04 \text{ \AA}$, $\nu = 5.0$ and $\alpha = 0.035 \text{ \AA}^{-1}$. For greater values of N , the gaussian ansatz tends to provide more binding than the exponential. For example, with the exponential ansatz, for $N = 16$ we get $E = -0.1816(7)$ K for $\alpha = 0.023 \text{ \AA}^{-1}$, and optimizing the different parameters one gets $E = -0.2514(6)$ K, with $b = 3.04 \text{ \AA}$. In conclusion, the gaussian wave function seems appropriate to be used as importance sampling in the DMC calculations.

III. DIFFUSION MONTE CARLO GROUND-STATE ENERGIES

Quantum Monte Carlo (QMC) methods provide the exact ground-state energy of a boson system, except for statistical errors. These techniques solve numerically the Schrödinger equation by means of a statistical simulation. They have been widely described in the literature, hence we briefly recall here the main ideas, referring the reader to Ref. 13 for a more detailed description on QMC techniques. In this work we use the diffusion Monte Carlo (DMC) method to solve the Schrödinger equation in imaginary time ($\tau = it$) for the function

$$f(\mathbf{R}, \tau) = \Phi_T(\mathbf{R})\Psi(\mathbf{R}, \tau) \quad (3)$$

where \mathbf{R} represents all the particle coordinates and is usually called walker, $\Psi(\mathbf{R}, \tau)$ is the wave function of the system, and $\Phi_T(\mathbf{R})$ is the previously determined trial wave function (Sect. II), used here as importance sampling. It is convenient to write the solution of the time-dependent Schrödinger equation in the following form

$$f(\mathbf{R}, \tau + \Delta\tau) = \int d\mathbf{R}' G(\mathbf{R}, \mathbf{R}', \Delta\tau) f(\mathbf{R}', \tau) \quad (4)$$

where G is the time-dependent Green's function and is formally written as

$$G(\mathbf{R}, \mathbf{R}'; \tau) = \langle \mathbf{R} | e^{-H\tau} | \mathbf{R}' \rangle \quad (5)$$

where H is the Hamiltonian of the system. The function $G(\mathbf{R}, \mathbf{R}'; \tau)$ represents the amplitude probability for the transition from an initial state \mathbf{R}' to a final one \mathbf{R} in a time τ . In the limit $\tau \rightarrow \infty$, Eq. (4) gives the exact ground-state wave function. Thus, knowing G for infinitesimal time steps $\Delta\tau$, the asymptotic solution for large times $f(\mathbf{R}, \tau \rightarrow \infty)$ can be obtained by solving iteratively the above equation. To this end, the exponential entering Eq. (5) is approximated to some fixed order in $\Delta\tau$. Both a linear and a quadratic DMC algorithm^{9,14} have been used in the present work, using the trial function Φ_T of Eq. (1) as guiding function. Our simulations have been carried out with a population of typically 400 walkers. As usual, some runs are first done to establish the asymptotic region of the short time propagator, then several values of the time step have been used, and finally a fit, either linear or quadratic, has been carried out to obtain the extrapolated energy. For example, for $N = 16$ the time steps 0.0001, 0.0002, 0.0003, and 0.0004 have been used to perform the extrapolation. In general, the statistical error is of the order of the time step error in our calculations.

In Table II we present the results of our linear DMC calculations of the total energy per particle for puddles containing N atoms. We have also reported the results of the binding energy per particle of the homogeneous 2D ${}^4\text{He}$ liquid at equilibrium density, $\rho_0^{DMC} = 0.04344 \text{ \AA}^{-2}$; both the energy per particle and the saturation density of the homogeneous system agree, within the statistical error, with those of Ref. 6, where the same version of the Aziz potential was used. We have also performed quadratic DMC calculations for some puddles, and found results which are compatible with the linear DMC ones within their error bars. For example, the quadratic algorithm provides $E_{\text{quad}} = -0.2612(2) \text{ K}$ for $N = 8$ and $-0.652(4)$ for $N = 64$. As expected, the DMC results lower the corresponding energies obtained by VMC either with our simple variational wave function or with a shadow wave function,⁷ by up to $\sim 25\%$ in the case of the bulk system. Indeed, for boson systems the DMC method provides exact ground-state energies, within statistical errors.

IV. ENERGY AND LINE TENSION

For a saturating self-bound system, the ground-state energy per particle can be expanded in a series of powers of the variable $N^{-1/D}$, where N is the number of constituents and D is the dimensionality of the space. This is the well-known mass formula, which in the present case writes

$$E(N)/N = \varepsilon_b + \varepsilon_l x + \varepsilon_c x^2 + \dots \quad (6)$$

with $x = N^{-1/2}$. The two first coefficients of this expansion are the bulk energy ε_b and the line energy ε_l , out of which the line tension λ is defined by $2\pi r_0 \lambda = \varepsilon_l$. Here r_0 is the unit radius, defined as the radius of a disk whose surface is equal to the inverse of the equilibrium density of the 2D bulk liquid, i.e. $\rho_0 \pi r_0^2 = 1$. Finally, ε_c is the so-called curvature energy.

Our calculated ground-state energies (Tables I and II) are plotted in Fig. 1 as a function of $N^{-1/2}$. One can see that the differences between our VMC and DMC energies increase with the number of atoms in the puddle. This clearly mirrors the simplicity of the trial wave function, which could be improved by including three-body correlations. Nevertheless this trial function is adequate for the importance sampling in the DMC calculation.

We have fitted these energies to a parabolic mass formula like Eq. (6). The coefficients of the fit are given in Table III, together with the deduced line tension. Although our VMC line tension is rather close to the previous estimation $\lambda = 0.07$ K/Å of Ref. 7, both VMC results are remarkably different from the DMC line tension. Notice that the DMC coefficient ε_b is identical, within statistical errors, to the bulk energy per particle of Table II. In fact, the χ^2 of the fit is very small, $\chi^2 = 5.7 \times 10^{-6}$.

To stress the curvature effect we have also plotted in the figure a straight line between the $N = 8$ and bulk DMC values. A linear fit of the DMC energies gives coefficients $\varepsilon_b = -0.885$ K and $\varepsilon_l = 1.80$ K, which are appreciably different from the previous ones. The bulk energy extrapolated from this linear fit differs from the directly calculated value, and the linear energy is closer to the variational one, thus giving a bad estimation for the linear tension. In all cases, the linear energy coefficient is approximately minus twice the volume energy term, similarly to the 3D case,¹¹ and therefore one expects curvature effects to be important. In both VMC and DMC cases the extracted ε_c is negative, i.e. the binding energy is a convex function of x as it also happens for the 3D clusters¹¹. This is in contrast with the value of ε_c reported in Ref. 7 which was positive.

V. DENSITY PROFILES

The calculation of observables given by operators that do not commute with the Hamiltonian poses a new problem in the DMC method. After convergence, the walkers are distributed according to the so-called mixed probability distribution given by the product of the exact and the trial wave functions. Therefore averaging the local values of the operator does not give the exact expectation value unless the operator commutes with the propagator. The result obtained by straightforward averaging is the mixed estimator which is of first order error in the trial wave function. Several options have been proposed in the literature in order to obtain unbiased (trial function independent and exact) values. We have checked that the mixed estimator of this work is very close to the extrapolated estimator, providing also the same qualitative behavior of the density profiles.

The DMC density profiles for several puddles are plotted in Fig. 2. The figure also contains an horizontal line which indicates the saturation density (ρ_0^{DMC}) of the homogeneous system. It can be seen that for the smaller clusters the central density is below ρ_0 , while for the larger values of N shown in the figure the central density is above ρ_0 , indicating a leptodermous behaviour. One expects that, increasing the number of particles, the central density will approach ρ_0 from above, as in the 3D case.^{15,16} It is worth noticing that very smooth surface oscillations appear for $N = 121$. A similar oscillating behaviour with larger amplitudes has been also observed in the 3D case¹⁶ already at smaller values of N .

The solid lines plotted in Fig. 2 are fits to our DMC densities provided by a generalized Fermi profile of the form:

$$\rho(r) = \frac{\rho_f}{\left(1 + \exp\left(\frac{r-R}{c}\right)\right)^\nu} \quad (7)$$

The parameters defining the Fermi profile are given in Table IV together with the thickness t and the root mean square (rms) radius $\langle r^2 \rangle^{1/2}$. The rms radius grows with the number of particles as $N^{1/2}$, as expected. Therefore it grows faster than in 3D, in which case grows as $N^{1/3}$. This behaviour allows for an alternative determination of the saturation density by performing a linear fit to the relation

$$\sqrt{\langle r^2 \rangle} = \sqrt{\frac{N}{2\pi\rho_0}} \quad (8)$$

The extracted value of ρ_0 from the mean square radius reported in Table IV is 0.0436 \AA^{-2} in good agreement with the determination from the calculation for the homogeneous system.

In the interval of N considered, the thickness t , defined as the distance over which the density falls from 0.9 of its value at origin to 0.1, is continuously increasing. However, as the finite value of the thickness for the semiinfinite system should define the asymptotic value of t , one expects that for larger puddles the thickness will probably have a maximum and smoothly approach this asymptotic value, as happens in the 3D case.¹⁵ Finally, one also realizes the asymmetric character of the density profiles with respect to the point at which the density falls at half its value at the origin. This can be appreciated by looking at the value of ν , which grows with N , and also to the increasing difference between the quantities R and $\langle r^2 \rangle^{1/2}$.

VI. SUMMARY AND CONCLUSIONS

In this work we have considered strictly two-dimensional systems of liquid ^4He , which are of course an idealization of a real quantum film. They are nevertheless interesting because their study can enlight the underlying structure of real quasi-2D systems. Of course, in the latter case, one has to take also into account the interaction with the substrate, which basically provides a global attractive potential. In the ideal 2D case, the suppression of the wave function component into the third dimension, produces an increment of the global repulsion between atoms, resulting in a smaller binding energy per particle, and a decrease of the equilibrium density.

The binding energies of two-dimensional ^4He clusters, calculated by means of a diffusion Monte Carlo method, are well fitted by a mass formula in powers of $x = N^{-1/2}$. The analysis of the mass formula provides the main result of this paper, namely the value of the line tension $\lambda = 0.121 \text{ K}/\text{\AA}$, which significantly differs from the one obtained from a similar analysis of VMC data and the one previously reported in the literature⁷. The quadratic term of the mass formula cannot be neglected and results in a negative value of the curvature energy as in the 3D case. The energy and the saturation density of the homogeneous system are in very good agreement with those given in Ref. 6.

The density profiles obtained with the extrapolated estimator have been fitted by a generalized Fermi function, and the behaviour of the rms radius and the thickness as well as the asymmetry character of the profile as a function of N have been discussed. However, calculations for larger puddles, which are out of the scope of the present paper due to

limitations in computing time, would be necessary to describe the complete N -dependence of the density profiles.

Acknowledgments

This work has been supported by DGICYT (Spain) project PB98-1247, DGI (Spain) grants BFM2001-0262 and BFM2002-00200, Generalitat de València grant GV01-216, Generalitat de Catalunya project 2001SGR00064, and MURST (Italy) grant MIUR-2001025498. J. M. P. acknowledges a fellowship from the Generalitat de Catalunya.

- ¹ See e.g. E. Krotscheck and J. Navarro (Eds.), *Microscopic Approaches to Quantum Liquids in Confined Geometries*, Series on Advances in Quantum Many-Body Theories, Vol. 4 (World Scientific, Singapore,2002).
- ² M. Bretz, J. G. Dash, D.C. Hickernell, E. O. McLean and O. E. Vilches, Phys. Rev. A **8**, 1589 (1973).
- ³ B. E. Clements, J. L. Epstein, E. Krotscheck and M. Saarela, Phys. Rev. B **48**, 7450 (1993).
- ⁴ C. E. Campbell and M. Schick, Phys. Rev. A **3**, 691 (1971).
- ⁵ P. A. Whitlock, G. V. Chester and M. H. Kalos, Phys. Rev. B **38**, 2418 (1988).
- ⁶ S. Giorgini, J. Boronat and J. Casulleras, Phys. Rev. B **54**, 6099 (1996).
- ⁷ B. Krishnamachari and G. V. Chester, Phys. Rev. B **59**, 8852 (1999).
- ⁸ R. A. Aziz, F. R. McCourt and C. C. K. Wong, Mol. Phys. **61**, 1487 (1987).
- ⁹ J. Boronat and J. Casulleras, Phys. Rev. B **49**, 8920 (1994).
- ¹⁰ J. Casulleras and J. Boronat, Phys. Rev. Lett. **84**, 3121 (2000).
- ¹¹ V. R. Pandharipande, S. C. Pieper and R. B. Wiringa, Phys. Rev. B **34** 4571 (1986).
- ¹² W. L. McMillan, Phys. Rev. **138**, A442 (1965).
- ¹³ B. L. Hammond, W. A. Lester Jr. and P. J. Reynolds, *Monte Carlo Methods in ab initio Quantum Chemistry*, Lecture and Course Notes in Chemistry, Vol. 1 (World Scientific, Singapore, 1994).
- ¹⁴ A. Sarsa, J. Boronat and J. Casulleras, J. Chem. Phys. **116** 5956 (2002).
- ¹⁵ S. Stringari and J. Treiner, J. Chem. Phys. **87** 5021 (1987).

¹⁶ S. A. Chin and E. Krotschek, Phys. Rev. B **45** 852 (1992).

TABLE I: Variational results for the ground-state energy per particle E/N of 2D ${}^4\text{He}$ puddles of various cluster sizes. The confining HO parameter α is given in \AA^{-1} and all energies are in K. The expectation values of the kinetic and the potential energies are also displayed. The column labelled KC refers to the VMC results of Ref. 7.

N	α	E/N	T/N	V/N	KC
8	0.1565	-0.2239(2)	1.3003(6)	-1.5242(5)	—
16	0.129	-0.3510(2)	1.7354(6)	-2.0864(5)	-0.380(8)
36	0.094	-0.4532(4)	2.031(3)	-2.484(3)	-0.471(7)
64	0.073	-0.4961(7)	2.159(2)	-2.655(2)	-0.528(5)
121	0.054	-0.5241(6)	2.223(2)	-2.747(2)	-0.570(7)
165	0.047	-0.5328(3)	2.289(1)	-2.822(1)	-0.602(7)
512	0.0266	-0.5493(5)	2.282(3)	-2.831(3)	-0.621(2)
∞	0.0000	-0.6904(8)	4.312(2)	-5.003(1)	—

TABLE II: Energy per particle (in K) for 2D ${}^4\text{He}$ puddles for various cluster sizes obtained with the linear DMC algorithm.

N	8	16	36	64	121	∞
E/N	-0.2613(4)	-0.4263(4)	-0.578(2)	-0.658(4)	-0.710(2)	-0.899(2)

TABLE III: Coefficients (in K) of a parabolic fit of the mass formula, as given in Eq. (6). The last column displays the deduced line tension (in K \AA^{-1}).

	ε_b	ε_l	ε_c	λ
VMC	-0.654	1.41	-0.62	0.083
Linear DMC	-0.897	2.06	-0.73	0.121

TABLE IV: Parameters of a Fermi-profile fit to the density profiles. All lengths are in Å and ρ_f is in Å^{-2} . The parameter ν is adimensional.

N	ρ_f	R	c	ν	t	$\langle r^2 \rangle^{1/2}$
8	0.03635	9.819	2.243	1.951	8.311	7.27
16	0.04197	14.80	2.971	3.153	10.27	9.27
64	0.04519	30.97	4.837	5.720	15.88	16.94
121	0.04474	41.80	5.805	6.311	18.95	22.82

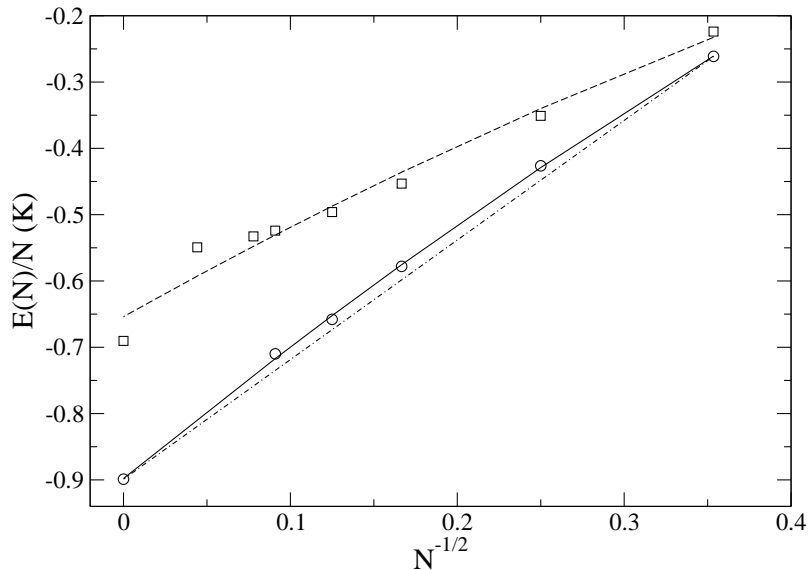


FIG. 1: Energies per particle (in K) of N -atom puddles as a function of $N^{-1/2}$, obtained from our VMC (squares) and DMC (circles) calculations. The interaction used is Aziz HFD-B(HE). Dashed and solid lines correspond to a least square fit to these energies. The dot-dashed line is a straight line between the $N = 8$ and bulk DMC values.

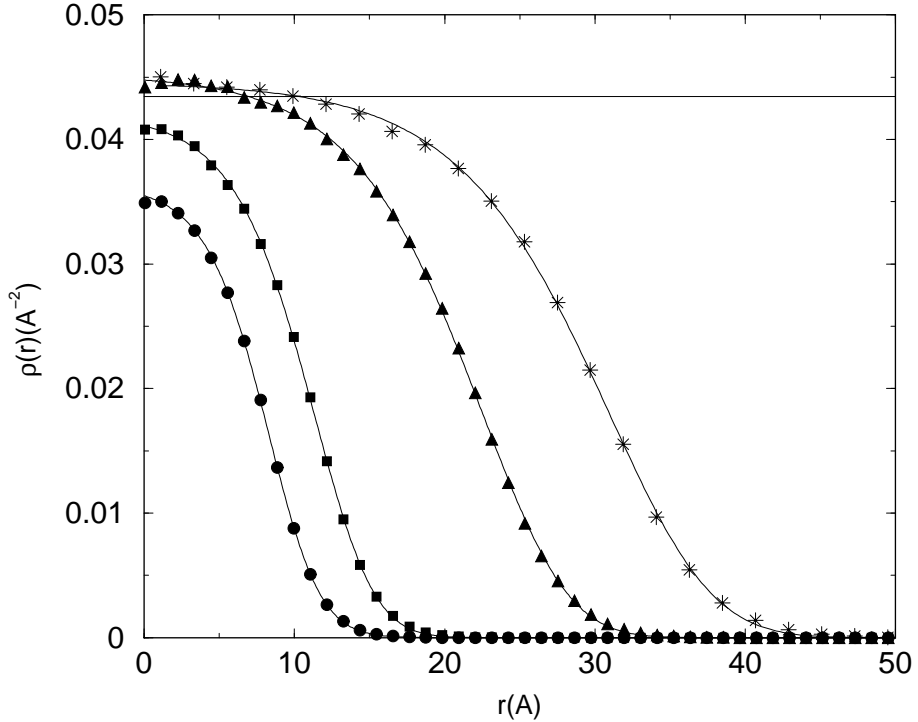


FIG. 2: Density profiles for ^4He puddles with various number of atoms, $N = 8$ (dots), 16 (squares), 64 (triangles) and 121 (stars), obtained from our linear DMC calculations. The solid horizontal line indicates the saturation density of the homogeneous system. The figure also contains the fits to the data provided by a generalized Fermi function, as explained in the text.